

# Coherent Dynamics of the Off-Diagonal Spin-Boson Model in the Ultra-Strong Coupling Regime

Nirmalendu Acharyya,<sup>1,\*</sup> Martin Richter,<sup>1,\*</sup> and Benjamin P. Fingerhut<sup>1,†</sup>

<sup>1</sup>*Max-Born-Institut für Nichtlineare Optik und Kurzzeitspektroskopie, D-12489 Berlin, Germany.*

(Dated: December 14, 2021)

Quantum mechanics describes the unitary time evolution of closed systems. In practice, every quantum system interacts with the environment leading to an irreversible loss of coherence. The Spin-Boson model (SBM) is central to the understanding of the fundamental process of decoherence of a two-state quantum system interacting with a bosonic heat bath but the nature of transient dynamics in the presence of hybrid diagonal and off-diagonal system-bath interactions remains largely unexplored. Here, we investigate how the hybrid system-bath interactions of an Ohmic environment induce localization in the bias-free SBM. For strong coupling to the environment, localization is strongly affected by a dynamically generated bias via the renormalization of the tunneling amplitude. We find that counteractive effects of Hamiltonian parameters on non-exponential short-time dynamics and long-time population equilibration can lead to a separation of timescales and non-equilibrium quantum coherent dynamics that can persist even for ultra-strong system-bath interaction. The findings offer novel opportunities to exploit coherence as a resource in quantum devices operating in the ultra-strong coupling regime.

PACS numbers: Valid PACS appear here

## I. INTRODUCTION

The Spin-Boson model (SBM) is paradigmatic for describing most important physical and chemical processes, like proton transfer in liquid phase [1], electron transfer and exciton transport in biological environments [2, 3] and tunneling in macroscopic two-state systems [4]. Despite its conceptual simplicity, distinct regimes of system-bath interaction strength  $\alpha$  characterize its complex dynamics and ground state properties. For Ohmic dissipation and low temperature ( $T \rightarrow 0$ ), coherent dynamics is observed at weak system-environment interaction strength ( $\alpha \lesssim \alpha_* \approx 0.5$ ) [5], mediated by tunneling amplitude  $\Delta_0$ . Incoherent decay arises for strong coupling to the environment ( $\alpha_* \lesssim \alpha \lesssim \alpha_c \approx 1 + O(\Delta_0/\omega_c)$ ) [6]. In both, the weak and strong coupling regime, the equilibrium ground state is delocalized. Ultra-strong coupling to the environment is realized for  $\alpha > \alpha_c$ . In this regime, the tunneling amplitude renormalizes to zero ( $\Delta_r \rightarrow 0$ ) and induces a freezing of the dynamics at initial configuration [7, 8]. As a consequence, the ground state in the ultra-strong coupling regime is localized, yielding the delocalized-to-localized BKT phase transition at  $\alpha = \alpha_c$  [5, 9, 10]. Recent realizations of the ultra-strong coupling regime of light-matter interaction [11–13] have spurred renewed interest in the SBM [8, 12, 14].

The environment affects the two-state quantum system of the SBM via the bath induced fluctuations of localized states (i.e. eigenstates of  $\sigma_z$ , cf. eq. 1), inducing population relaxation and dephasing [15]. The influence of

non-diagonal system-bath interactions on the tunneling amplitude  $\Delta_0$  is less well understood. Early work by Laird, Budimir, and Skinner investigated a model of two nondegenerate quantum states coupled linearly and off-diagonally to a bath [16]. Their findings of strictly non-zero population excitation rates were later confirmed by Reichman and Silbey [17]. Ground state properties of the off-diagonal SBM have been investigated [18–20]. Particular importance of diagonal and off-diagonal contributions to the system-bath interaction was demonstrated recently via the finding of persistent steady state coherences in absence of a bare tunneling amplitude  $\Delta_0$  [18].

The nature of the transient dynamics in presence of hybrid diagonal and non-diagonal system-bath interaction remains largely unexplored. Here, we demonstrate the emergence of coherent dynamics facilitated by hybrid system-bath interactions that can persist even for ultra-strong coupling to the environment. We start by describing the numerical treatment of the off-diagonal SBM with hybrid system-environment interactions (Sec. II). Equilibrium localization is analyzed for high and low temperature in Sec. III, revealing counteractive effects of Hamiltonian parameters on non-exponential short-time dynamics and long-time population equilibration. Exploiting the counteractive control parameters, a timescale separation in short and long-time dynamics can impose quantum coherent dynamics even at ultra-strong system-bath interaction (Sec. IV). Oscillation frequency and dephasing behavior are rationalized with help of the off-diagonal primary reaction coordinate (PRC) model that facilitates analytical access in the limit of ultra-slow dissipation

\*Current Address: Institut für Physikalische Chemie, Friedrich-Schiller-Universität Jena, D-07743 Jena, Germany

†Electronic address: fingerhut@mbi-berlin.de

## II. OFF-DIAGONAL SPIN BOSON MODEL

We consider the symmetric SBM where a degenerate two-state (spin) system interacts bi-linearly with a harmonic reservoir via diagonal and off-diagonal interactions

$$H = \frac{\Delta_0}{2} \sigma_x + \sum_i \omega_i a_i^\dagger a_i + \frac{bI + \cos \varphi \sigma_z + \sin \varphi \sigma_x}{2} \sum_i c_i X_i. \quad (1)$$

Here,  $\sigma_\alpha$  with  $\alpha = x, z$  denote Pauli matrices and  $a_i (a_i^\dagger)$  are annihilation (creation) operators of bosonic modes with frequencies  $\omega_i$  and  $X_i = a_i + a_i^\dagger$ . The mixing angle  $\varphi$  interpolates between pure diagonal ( $\varphi = 0$ ) and pure off-diagonal ( $\varphi = \pi/2$ ) coupling to the environment. The term  $bI \sum_i c_i (a_i + a_i^\dagger)$  shifts the origin of bath oscillators and controls their equilibrium displacement. It is well understood that for diagonal coupling to the environment ( $\varphi = 0$ ) and ergodic system-environment dynamics initial preparation effects via parameter  $b$  are insignificant. In absence of initial system-bath correlations, the system relaxes to thermal equilibrium independent of the initially prepared state [15]. As we will show, the term  $bI \sum_i c_i (a_i + a_i^\dagger)$  takes a crucial role in affecting non-equilibrium dynamics for  $\varphi \neq 0$ .

The environment is characterized by the spectral density  $J(\omega) \equiv \frac{\pi}{2} \sum_j \frac{c_j^2}{m_j \omega_j} \delta(\omega - \omega_j)$ . We consider Ohmic dissipation with Lorentzian high frequency cut-off,  $J(\omega) = 2\pi\alpha\omega\omega_c^2/(\omega^2 + \omega_c^2)$ , where  $\alpha$  characterizes the system-bath interaction strength and the cut-off frequency  $\omega_c$  is related to the inverse of Drude memory time  $\tau_D = 1/\omega_c$  [8, 15].

Observables are determined by the reduced density matrix  $\tilde{\rho}(t) = \text{Tr}_B [e^{-iHt} \rho(0) e^{iHt}]$ . Employing factorized initial conditions and assuming the bath in thermal equilibrium,  $\tilde{\rho}(t)$  was evaluated numerically for initial condition  $\tilde{\rho}(0) = |+\rangle\langle+|$  ( $|\pm\rangle$  denote eigenstates of  $\sigma_z$ ) with the non-perturbative quasi-adiabatic propagator path integral method [21–23]. Mask assisted coarse graining of influence coefficients (MACGIC-QUAPI) [24] facilitates access to long-time non-Markovian system-bath correlations. The algorithm exploits a finite memory time  $\tau_M \propto \tau_D$  characterizing non-Markovian memory time scale and uses a coarse grained representation of the influence functional (represented by mask of size  $k_{eff}$ ) for computational efficiency. By decreasing the size of the Trotter time-step  $\Delta t$  and increasing memory time  $\tau_M = \Delta k_{max} \Delta t$  convergence to numerically exact results is obtained via an increase in the number of coarse grained quadrature points ( $k_{eff} \rightarrow \Delta k_{max}$ ) and a decrease in filter threshold ( $\theta \rightarrow 0$ ), details are given in Refs. 24, 25 (see SI for convergence of numerical simulations).

## III. EQUILIBRIUM LOCALIZATION WITH OFF-DIAGONAL SYSTEM-ENVIRONMENT INTERACTIONS

Fig.1a demonstrates the impact of hybrid system-environment interaction on non-equilibrium dynamics in the strong coupling regime at high temperature ( $\alpha \gtrsim \alpha_*(T) \approx \Delta_r/(\pi k_B T)$ ,  $k_B T \gtrsim \Delta_r$  with renormalized tunneling amplitude  $\Delta_r$  [5]). Two distinct dynamical regimes can be identified: ultra-fast universal decoherence is reflected in non-exponential decay [26–28] and is followed by relatively slower long-time equilibration dynamics. The amplitude of ultra-fast non-exponential decay shows pronounced sensitivity to the non-diagonal interaction ( $\varphi \neq 0$ ). It is apparent from Fig.1a that the off-diagonal system-environment interaction ( $\varphi \neq 0$ ) also affects the equilibrium ground state  $P_z(t \rightarrow \infty)$ , i.e., the system equilibrates to a localized state ( $P_z(t \rightarrow \infty) \neq 0$ ) even in absence of a bare bias (cf. eq.1). In principle, two distinct effects determine equilibrium localization: (i) an effective bias  $\hat{\epsilon} = \Delta_0 \sin \varphi$  is generated via a rotation of basis due to non-diagonal system environment interaction [30, 31] (see also SI, eq. S1-S3); (ii) renormalization of the tunneling amplitude  $\Delta_0$  due to the strong interaction with the environment affects the dressed Hamiltonian [15]. *A priori*, the relevance and interdependence of both effects is unclear and has not been explored numerically.

We find that  $P_z(t \rightarrow \infty)$  shows a strong dependence on  $\varphi$  and increases with coupling strength  $\alpha$  (Fig.1d). Localization for  $\varphi \neq 0$  is determined by the amplitude of ultra-fast non-exponential decay and long-time exponential dynamics. The latter is characterized by the population relaxation rate  $\hat{\Gamma}$  which decreases with increasing  $\alpha$  [15] and additionally is a non-monotonic function of  $\varphi$  that decreases as  $\varphi \rightarrow \pi/2$  (Fig.1b). The pure dephasing case is realized for  $\varphi = \pi/2$  where the tunneling amplitude, and consequently  $\hat{\Gamma}$  vanishes.

Equilibrium localization was analyzed by extending a generalized master equation approach [5, 29] to derive approximate solutions of exponential long-time dynamics in presence of diagonal and non-diagonal system-environment interaction ( $\varphi \neq 0$ ). We therefore unitarily transform the Hamiltonian (eq.1)  $H \rightarrow \hat{H} = U^\dagger H U$  with  $U = \exp(-i\frac{\varphi}{2}\sigma_y)$ , where  $U$  diagonalizes the system-bath interaction [30].  $\hat{H}$  takes the form of the ordinary SBM with transformed initial conditions and transformed parameters  $\hat{\epsilon} = \Delta_0 \sin \varphi$  and  $\hat{\Delta} = \Delta_0 \cos \varphi$ . Note that  $U$  is defined in space of system-bath interaction and does not necessarily diagonalize the system part of eq. 1 as both contributions to the total Hamiltonian do not commute. Approximate solutions for long-time dynamics were obtained in transformed basis, followed by reverse transformation. In the overdamped regime this yields exponential dynamics

$$P_z(t) \approx (A - B \tanh(-\beta E/2)) e^{-\hat{\Gamma} t} + B \tanh(-\beta E/2) \quad (2)$$

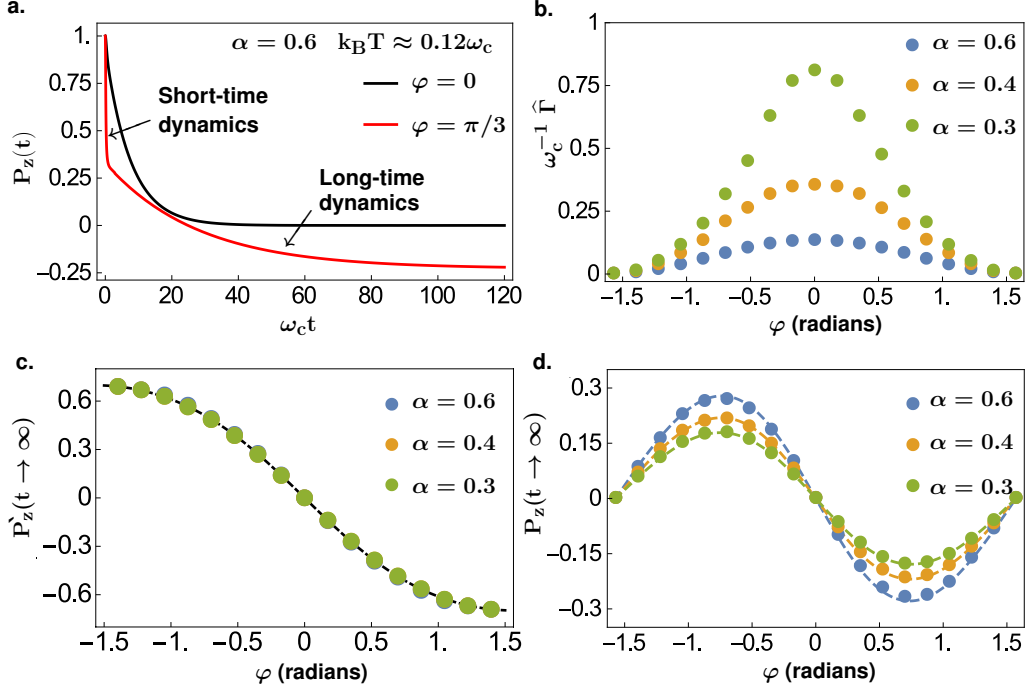


FIG. 1: **a.** Impact of hybrid system-bath interaction on short-time and long-time dynamics: population difference  $P_z(t) = \text{Tr}_B[\sigma_z \hat{\rho}(t)]$  for diagonal ( $\varphi = 0$ ) and hybrid diagonal and off-diagonal coupling ( $\varphi \neq 0$ ) in the overdamped regime ( $\alpha > \alpha_*(T)$ ), see SI for non-equilibrium dynamics at weak system-bath interaction and  $\varphi = 0$  ( $\alpha \lesssim \alpha_*(T) \approx \Delta_r/(\pi k_B T)$ ). **b.** Population relaxation rate  $\hat{\Gamma}$  for varying system-bath interaction strengths  $\alpha$ ,  $\hat{\Gamma}$  is obtained via an exponential fit of the late-time dynamics (see SI). **c.** Population difference  $P'_z(t \rightarrow \infty)$  in intermediate, transformed basis (cf. SI, eq. S.1-S.3) as function of mixing angle  $\varphi$  and for various values of  $\alpha$  (dots). The dashed line gives the analytical results with effective bias  $\hat{\epsilon} = \Delta_0 \sin \varphi$  due to basis rotation. Note that numerical values for varying  $\alpha$  almost perfectly coincide. **d.**  $P_z(t \rightarrow \infty)$  as function of mixing angle  $\varphi$  and for various values of  $\alpha$ , dots and dashed lines represent numerical data and analytical results (eq.3 with  $F = (\omega_c \beta)^{-\alpha}$ ), respectively. Simulations are performed at  $k_B T \approx 0.12 \omega_c \approx \Delta_r$  ( $T = 100$  K) and  $\Delta_0 = 0.2 \omega_c$ ,  $b = 0$ , cf. SI, Table S1.

with amplitudes

$$A = \frac{(1-F)^2 \sin^2 \varphi \cos^2 \varphi}{\sin^2 \varphi + F^2 \cos^2 \varphi}, \quad B = \frac{(1-F) \sin \varphi \cos \varphi}{\sqrt{\sin^2 \varphi + F^2 \cos^2 \varphi}} \quad (3)$$

where  $E \equiv \sqrt{\hat{\epsilon}^2 + \hat{\Delta}_r^2}$ ,  $\beta \equiv 1/(k_B T)$  and  $F \equiv \hat{\Delta}_r/\Delta_0$  (see SI for derivation).

From eq. 2-3 we find that equilibrium localization amplitude  $P_z(t \rightarrow \infty) = B \tanh(-\beta E/2)$  crucially depends on the renormalization factor  $F$ . In the weak coupling regime the renormalization effect is weak ( $F \approx 1$ ) and  $B$  is vanishingly small. Thus, localization in absence of a bare bias arises due to a dynamically generated bias via the renormalized tunneling amplitude  $\hat{\Delta}_r$  at strong coupling to the environment. We note that the dynamically generated bias is distinct from the bias  $\hat{\epsilon}$  due to rotation of bare Hamiltonian parameters. This becomes evident from the fact that localization does not maximize near  $\varphi = \pi/2$ , instead at high temperature we find that  $P_z(t \rightarrow \infty)$  maximizes near  $\varphi = \pi/4$  (Fig. 1d). For comparison, Fig. 1c show the population difference  $P'_z(t \rightarrow \infty)$  in intermediate, transformed basis with the effective bias  $\hat{\epsilon}$  due to rotation of bare Hamiltonian where localization maximizes for  $\varphi = \pi/2$  [15, 31]. Excellent agreement is found for  $P_z(t \rightarrow \infty)$  obtained from numerical simulations and as predicted by eq. 3

where the renormalization effect via  $F$  is taken into account (Fig. 1d, see also SI, Fig. S3 for  $P_x(t \rightarrow \infty)$  dependence on  $\varphi$ ). At high temperature and strong coupling,  $\hat{\Delta}_r = \hat{\Delta}(\omega_c \beta)^{-\alpha}$  [32, 33] which yields a non-zero decay rate  $\hat{\Gamma} \propto \Delta_0^2 \cos^2 \varphi (\omega_c \beta)^{-2\alpha}$  and further confirms the numerically observed behavior (Fig. 1b).

In the off-diagonal case at low temperature ( $\varphi \neq 0$ ,  $k_B T \rightarrow 0$ ), the finite population relaxation rate  $\hat{\Gamma}$  prevails at weak and strong coupling due to a non-vanishing renormalized tunneling amplitude  $\hat{\Delta}_r = \hat{\Delta}(\hat{\Delta}/\omega_c)^{\alpha/(1-\alpha)}$  [5, 32]. Nevertheless, eqs. 2-3 predict localization for  $\varphi \neq 0$  ( $P_z(t \rightarrow \infty) \approx B \tanh(-\beta E/2) \neq 0$  with  $\hat{\Delta}_r = \hat{\Delta}(\hat{\Delta}/\omega_c)^{\alpha/(1-\alpha)}$ ) that was confirmed numerically (Fig. 2b). Such findings contrast with the localization behavior induced by the effective bias  $\hat{\epsilon} = \Delta_0 \sin \varphi$  generated via basis rotation (Fig. 2a) and the bias-free SBM ( $\varphi = 0$ ) subject to Ohmic dissipation that shows delocalization in weak and strong coupling regimes ( $P_z(t \rightarrow \infty) = 0$  for  $\alpha \lesssim \alpha_* \approx 0.5$  and  $\alpha_* \lesssim \alpha \lesssim \alpha_c \approx 1 + O(\Delta_0/\omega_c)$  [6]).

At ultra-strong coupling and low temperature the tunneling amplitude renormalizes to zero for  $\varphi = 0$  ( $\Delta_r \rightarrow 0$ ,  $\alpha \gtrsim \alpha_c \approx 1 + O(\Delta_0/\omega_c)$ ,  $k_B T \rightarrow 0$ ) [7, 8] which leads to freezing of the population at the initial configuration and formation of a localized phase.[6] For  $\varphi \neq 0$ ,  $\Delta_r \rightarrow 0$  be-

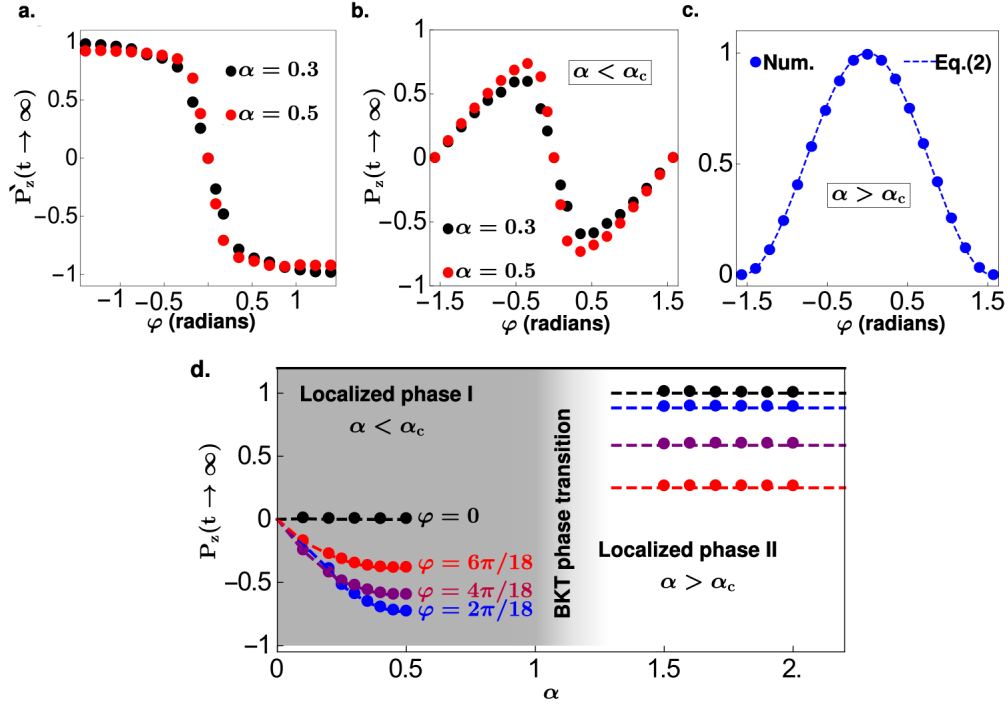


FIG. 2: (a.) Population difference  $P'_z(t \rightarrow \infty)$  in intermediate, transformed basis (cf. SI, eq. S.1-S.3) as function of mixing angle  $\varphi$  at low  $T \rightarrow 0$  for  $\alpha < \alpha_c$ .  $P_z(t \rightarrow \infty)$  as a function of  $\varphi$  at low  $T \rightarrow 0$  for  $\alpha < \alpha_c$  (b.) and  $\alpha > \alpha_c$  (c.). Dots and dashed line mark numerical and analytical results (eq.3 with  $F = 0$ ), respectively. d. Sketch of the localized-to-localized phase transition in the off-diagonal SBM. Phase I ( $\alpha < \alpha_c$ ) shows finite values of  $P_z(t \rightarrow \infty)$  for  $\varphi \neq 0$  and dependence on  $\alpha$ ,  $\varphi$ , and  $\Delta_0/\omega_c$ . In phase II ( $\alpha > \alpha_c$ ),  $P_z(t \rightarrow \infty)$  is determined by  $\varphi$  but independent of  $\alpha$  and  $\Delta_r$ . In numerical simulations  $\Delta_0/\omega_c = 0.1$ ,  $b = 0$  and  $k_B T \approx 0.0003\omega_c$  ( $T \approx 0.05K$ ), cf. SI, Table S2-S5.

havior is preserved ( $F = 0$ , eq.3) beyond the same value of  $\alpha_c$  [48]. Accordingly,  $\hat{\Gamma} \rightarrow 0$  for  $\alpha > \alpha_c$  and the mechanism leading to freezing of the dynamics in the SBM [9, 10] is conserved for  $\varphi \neq 0$ . Localization amplitude  $P_z(t \rightarrow \infty) = A = \cos^2 \varphi$  (obtained upon inserting  $\hat{\Gamma} = 0$  and  $F = 0$  in eq.3) is confirmed with excellent accuracy in numerical simulations (Fig.2c).

As a first important result we thus find a BKT phase transition for  $\alpha \approx \alpha_c$  and all values of  $\varphi$ , however, for  $\varphi \neq 0$  the transition is between distinct localized phases I and II (Fig.2d) with different localization mechanism and ground state. In phase I ( $\alpha < \alpha_c$ ), equilibrium properties depend on  $\Delta_0/\omega_c$ ,  $\alpha$  and  $\varphi$ . Localization arises due to a dynamically generated bias via the renormalization of  $\hat{\Delta}_r$  transcending behavior of the SBM in the weak coupling regime. In phase II ( $\alpha > \alpha_c$ )  $\Delta_0/\omega_c$  become irrelevant. Localization sensibly depends on  $\varphi$  but is found to be independent of  $\alpha$  [49]. In both phases, the term  $bI \sum_i c_i(a_i + a_i^\dagger)$  (eq.1) has no effect on long-time dynamics, i.e.,  $\hat{\Gamma}$  and  $P_z(t \rightarrow \infty)$ .

The population relaxation rate  $\hat{\Gamma}$  decreases with increasing  $\alpha$  and  $\varphi \rightarrow \pi/2$  (Fig.1b). In contrast, we observe for any temperature an acceleration of short-time dynamics as  $\alpha$  increases and  $\varphi \rightarrow \pi/2$  (SI, Fig.S4). Such counteractive effects of  $\alpha$  and  $\varphi$  on short- and long-time dynamics can be exploited for control of dynamics be-

yond the scope of the ordinary SBM with Ohmic dissipation.

#### IV. COHERENT DYNAMICS AT ULTRA-STRONG SYSTEM-ENVIRONMENT INTERACTION

Fig.3 presents non-equilibrium dynamics of the off-diagonal SBM ( $\varphi \neq 0$ ) with ultra-strong coupling ( $\alpha > \alpha_c$ ,  $k_B T \approx 0.0003\omega_c$ ). For diagonal system-bath interaction ( $\varphi = 0$ ) the dynamics remains frozen in the initial configuration. In contrast, for  $\varphi \neq 0$  nontrivial short-time dynamics precedes freezing of dynamics for  $\alpha > \alpha_c$ . Interestingly, such short-time dynamics can be oscillatory for  $\varphi \neq 0$  and  $b \neq 0$ , despite the ultra-strong interaction strength (Fig.3a,b). At the origin of oscillatory short time dynamics is a timescale separation, i.e., particularly fast short-time dynamics and slow long-time equilibration due to counteractive effects of parameters  $\alpha$ ,  $\varphi$  and  $b$  on system, interaction and bath part of the Hamiltonian (eq. 1). Universal decoherence [27] imposes non-exponential short-time dynamics that is independent of the system Hamiltonian but strongly affected by the details of the system bath interaction and the bath ( $\alpha$ ,  $\tan \varphi$  and  $b$ ). For any temperature we observe acceleration of the short-time dynamics as  $\alpha$  increases,  $\varphi$  ap-

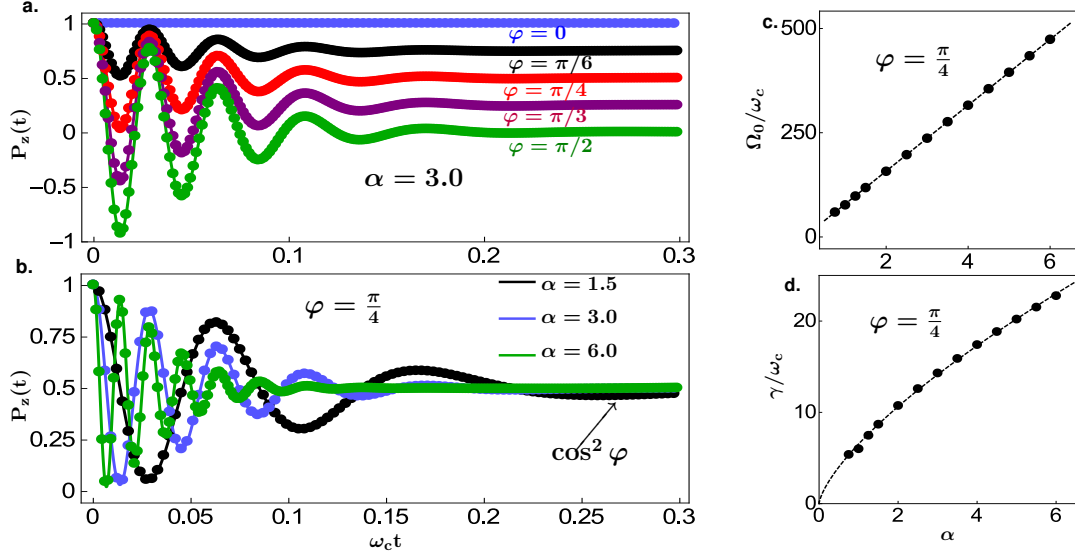


FIG. 3: Non-equilibrium dynamics at low temperature in the ultra-strong coupling regime ( $\alpha > \alpha_c$ ) for various values  $\varphi$  (a.) and  $\alpha$  (b.). Solid lines represent MACGIC-QUAPI simulations and dots mark OFP simulations (see SI). Dependence of oscillation frequency  $\Omega_0$  (c.) and damping constant  $\gamma$  (d.) on coupling strength  $\alpha$ . In all simulations  $\Delta_0 = 0.1\omega_c$ ,  $b = 4$  and  $T \approx 0.05K$ , cf. SI, Table S6.

proaches  $\pi/2$  and  $b$  increases (SI, Fig.S4). Parameter  $b$  of the bath Hamiltonian is thus a new relevant parameter for the off-diagonal SBM. Conversely,  $\alpha$  and  $\varphi$  affect the system dynamics (population relaxation and dephasing) via basis rotation and renormalization of tunneling amplitude  $\Delta_0$ .

Observed dynamics exhibits the following characteristics: (i) the oscillation amplitude sensibly depends on  $\varphi$  (Fig.3a); (ii) the oscillation frequency increases linearly with increasing  $\alpha$  (Fig.3b,c) and  $b$  (SI, Fig.S6); (iii) short-time dynamics is independent of  $\Delta_0/\omega_c$  and insensitive to a further lowering of  $T$  (SI, Fig.S5) which reflects the quantum coherent origin of universal decoherence for  $\varphi \neq 0$ . The oscillatory dynamics has thus a fundamentally different origin than the one observed in the weak coupling regime ( $\alpha < \alpha_*$ ) where oscillation frequency is determined by  $\Delta_r$ .

We find that the fit-function

$$P_z(t) \approx \cos^2 \varphi + \sin^2 \varphi \cos(\Omega_0 t + \Omega_1 t^2 + \Omega_2 t^3) e^{-\gamma^2 t^2} \quad (4)$$

accurately describes the dynamics. The  $\cos^2 \varphi$  term accounts for long-time behavior ( $P_z(t \rightarrow \infty)$ ),  $\Omega_0$  describes the leading order oscillation frequency,  $\Omega_{1,2}$  account for temporal modulation of  $\Omega_0$  and  $\sin^2 \varphi$  determines the amplitude. The latter vanishes for  $\varphi = 0$  rendering off-diagonal coupling necessary for emerging coherences. A fit of the dynamics reveals a linear increase of  $\Omega_0$  with  $\alpha$  ( $\Omega_0 \propto b\alpha\omega_c$ , Fig.3c) which partially resembles oscillatory behavior of sub-Ohmic environments [34]. Oscillations decay with  $\exp[-\gamma^2 t^2]$  where damping constant  $\gamma$  increases sub-linearly with  $\alpha$  ( $\gamma = \gamma_0 \alpha^k \omega_c$  with  $k \approx 0.7$ ; Fig.3d), thus, forming the essence of persistence of oscillations for increasing  $\alpha$  (Fig.3b). The observed sub-exponential damping is distinct from the reported super-exponential to algebraic decay for diagonal system bath

interaction [28].

Microscopic origin of oscillatory short-time dynamics was rationalized via a off-diagonal PRC model that couples electronic states  $|\pm\rangle$  to a primary coordinate  $Q$  that in turn couples to a dissipative Ohmic environment [35–37]:

$$\begin{aligned} \mathcal{H} &= \frac{1}{2} \Delta_0 \sigma_x + \hat{\Omega}^2 \frac{\kappa}{2} (\cos \varphi \sigma_z + \sin \varphi \sigma_x + b) Q + \mathcal{H}_Q + \mathcal{H}_B \\ \mathcal{H}_B &= \sum_{j=0}^{\infty} \left[ \frac{p_j^2}{2m_j} + \frac{1}{2} m_j \omega_j^2 \left( q_j - \frac{g_j Q}{m_j \omega_j^2} \right)^2 \right] \end{aligned} \quad (5)$$

and  $\mathcal{H}_Q = \frac{1}{2} (P^2 + \hat{\Omega}^2 Q^2)$ . Canonical transformation  $Q = \sum_j v_j q_j$  allows to map eq.5 onto the off-diagonal SBM (eq.1) [38] with  $\tan \varphi$  being a measure of non-Condon effects [39, 40].

In the limit of ultra-slow dissipation (ultra-strong coupling), the approximate time-evolution of a vibronic wavepacket in the PRC (eq.5) confirms the leading order oscillatory behavior (cf. SI for analytical treatment). The oscillation frequency  $\Omega_0$  grows linearly with  $b\alpha$ , the amplitude of the leading order term being  $\sin^2 \varphi$  that is damped via  $\gamma$  which shows sub-linear dependence on  $\alpha$ .

## V. CONCLUSIONS

The close agreement between analytical and numerical findings suggests a picture where oscillatory dynamics, preserved in the ultra-strong coupling regime, arises via non-Condon effects mediated by a PRC contained in

the Ohmic spectral density. This suggests a dominant short-time relaxation channel of the off-diagonal SBM where the initially excited state strongly interacts with mode  $Q$ . From the perspective of the SBM this implies that at ultra-strong coupling in the short-time regime the system interacts primarily with a few bath modes. The finite (non-Markovian) relaxation timescale of the Ohmic spectral density constitutes a “sluggish” environment and prevents uniform dissipation, thus, imposing a separation of timescales. The non-equilibrium state of the PRC is prevented from instantaneous dissipation into the bath and the electronic system becomes susceptible to re-excitation, resulting in oscillatory short-time dynamics that can not be rationalized via bare tunneling amplitude  $\Delta_0$ . The particular high efficiency of the off-diagonal mediated dissipation channel has far reaching relevance for ultrafast condensed phase (molecular) relaxation where the importance of non-Condon effects was stressed in molecular vibronic photo-relaxation [41–43] [50].

The prediction of quantum coherent dynamics in the ultra-strong coupling regime is readily amenable to ex-

perimental verification in various platforms [12]. In circuit QED, the ultra-strong coupling regime with strong system-bath entanglement was demonstrated [14] and control over the longitudinal-to-transverse coupling ratio  $\tan \varphi$  is provided via Josephson and charging energies; experimental manipulation of the displacement parameter  $b$  can be achieved via the gate charge [44]. SQUID devices [4] provide access to variations of  $\Delta_0$  and thus control over the amplitude of off-diagonal induced steady state coherences and localization in the weak and strong coupling regime.

## ACKNOWLEDGMENTS

This research has received funding from the European Research Council (ERC) under the European Union’s Horizon 2020 research and innovation program (grant agreement No. 802817). B.P.F. acknowledges support by the DFG within the Emmy-Noether Program (Grant No. FI 2034/1-1).

- 
- [1] R. I. Cukier and M. Morillo, *J. Chem. Phys.* **91**, 857 (1989).
  - [2] D. Xu and K. Schulten, *Chem. Phys.* **182**, 91 (1994).
  - [3] M. Thorwart, J. Eckel, J. Reina, P. Nalbach, and S. Weiss, *Chem. Phys. Lett.* **478**, 234 (2009).
  - [4] S. Han, J. Lapointe, and J. E. Lukens, *Phys. Rev. Lett.* **66**, 810 (1991).
  - [5] A. J. Leggett, S. Chakravarty, A. T. Dorsey, M. P. A. Fisher, A. Garg, and W. Zwerger, *Rev. Mod. Phys.* **59**, 1 (1987).
  - [6] A. Strathearn, P. Kirton, D. Kilda, J. Keeling, and B. W. Lovett, *Nat. Commun.* **9**, 3322 (2018).
  - [7] P. W. Anderson, G. Yuval, and D. R. Hamann, *Phys. Rev. B* **1**, 4464 (1970).
  - [8] L. Magazzù, P. Forn-Díaz, R. Belyansky, J. L. Orgiazzi, M. A. Yurtalan, M. R. Otto, A. Lupascu, C. M. Wilson, and M. Grifoni, *Nat. Commun.* **9**, 1403 (2018).
  - [9] A. J. Bray and M. A. Moore, *Phys. Rev. Lett.* **49**, 1545 (1982).
  - [10] S. Chakravarty, *Phys. Rev. Lett.* **49**, 681 (1982).
  - [11] A. Wallraff, D. I. Schuster, A. Blais, L. Frunzio, R. S. Huang, J. Majer, S. Kumar, S. M. Girvin, and R. J. Schoelkopf, *Nature* **431**, 162 (2004).
  - [12] A. Frisk Kockum, A. Miranowicz, S. De Liberato, S. Savasta, and F. Nori, *Nat. Rev. Phys.* **1**, 19 (2019).
  - [13] P. Forn-Díaz, L. Lamata, E. Rico, J. Kono, and E. Solano, *Rev. Mod. Phys.* **91**, 025005 (2019).
  - [14] P. Forn-Díaz, J. J. García-Ripoll, B. Peropadre, J. L. Orgiazzi, M. A. Yurtalan, R. Belyansky, C. M. Wilson, and A. Lupascu, *Nat. Phys.* **13**, 39 EP (2016).
  - [15] U. Weiss, *Quantum Dissipative Systems; 4th ed.* (World Scientific, Singapore, 2012).
  - [16] B. B. Laird, J. Budimir, and J. L. Skinner, *J. Chem. Phys.* **94**, 4391 (1991).
  - [17] D. R. Reichman and R. J. Silbey, *J. Chem. Phys.* **104**, 1506 (1996).
  - [18] G. Guarnieri, M. Kolář, and R. Filip, *Phys. Rev. Lett.* **121**, 070401 (2018).
  - [19] Y. Zhao, Y. Yao, V. Chernyak, and Y. Zhao, *J. Chem. Phys.* **140**, 161105 (2014).
  - [20] N. Zhou, L. Chen, D. Xu, V. Chernyak, and Y. Zhao, *Phys. Rev. B* **91**, 195129 (2015).
  - [21] N. Makri and D. E. Makarov, *J. Chem. Phys.* **102**, 4611 (1995).
  - [22] E. Sim and N. Makri, *Comput. Phys. Commun.* **99**, 335 (1997).
  - [23] E. Sim, *J. Chem. Phys.* **115**, 4450 (2001).
  - [24] M. Richter and B. P. Fingerhut, *J. Chem. Phys.* **146**, 214101 (2017).
  - [25] M. Richter and B. P. Fingerhut, *Faraday Discuss.* **216**, 72 (2019).
  - [26] D. E. Makarov and N. Makri, *Chem. Phys. Lett.* **221**, 482 (1994).
  - [27] D. Braun, F. Haake, and W. T. Strunz, *Phys. Rev. Lett.* **86**, 2913 (2001).
  - [28] J. Tuorila, J. Stockburger, T. Ala-Nissila, J. Ankerhold, and M. Möttönen, *Phys. Rev. Research* **1**, 013004 (2019).
  - [29] M. Grifoni, E. Paladino, and U. Weiss, *Eur. Phys. J. B* **10**, 719 (1999).
  - [30] Z. Lü, L. Duan, X. Li, P. M. Shenai, and Y. Zhao, *J. Chem. Phys.* **139**, 164103 (2013).
  - [31] V. Romero-Rochin and I. Oppenheim, *Physica A* **155**, 52 (1989).
  - [32] T. A. Costi and G. Zaránd, *Phys. Rev. B* **59**, 12398 (1999).
  - [33] T. Ruokola and T. Ojanen, *Phys. Rev. B* **83**, 045417 (2011).
  - [34] D. Kast and J. Ankerhold, *Phys. Rev. Lett.* **110**, 010402 (2013).
  - [35] A. Garg, J. Onuchic, and V. Ambegaokar, *J. Chem. Phys.*

- 83**, 4491 (1985).
- [36] N. Lambert, S. Ahmed, M. Cirio, and F. Nori, *Nat. Commun.* **10**, 3721 (2019).
  - [37] L. A. Correa, B. Xu, B. Morris, and G. Adesso, *J. Chem. Phys.* **151**, 094107 (2019).
  - [38] V. Chernyak and S. Mukamel, *J. Chem. Phys.* **105**, 4565 (1996).
  - [39] M. G. Mavros, D. Hait, and T. Van Voorhis, *J. Chem. Phys.* **145**, 214105 (2016).
  - [40] W. Domcke, D. R. Yarkony, and H. Köppel, *Conical Intersections*, Advanced Series in Physical Chemistry (World Scientific, 2004).
  - [41] H. Tamura, R. Martinazzo, M. Ruckebauer, and I. Burghardt, *J. Chem. Phys.* **137**, 22A540 (2012).
  - [42] N. Christensson, H. F. Kauffmann, T. Pullerits, and T. Mančal, *J. Phys. Chem. B* **116**, 7449 (2012).
  - [43] C. Schnedermann, A. M. Alvertis, T. Wende, S. Lukman, J. Feng, F. A. Y. N. Schröder, D. H. P. Turban, J. Wu, N. D. M. Hine, N. C. Greenham, et al., *Nat. Commun.* **10**, 4207 (2019).
  - [44] A. Blais, R.-S. Huang, A. Wallraff, S. M. Girvin, and R. J. Schoelkopf, *Phys. Rev. A* **69**, 062320 (2004).
  - [45] S. Florens, D. Venturelli, and R. Narayanan, *Quantum Phase Transition in the Spin Boson Model* (Springer, Berlin, Heidelberg, 2010), pp. 145–162.
  - [46] P. Hamm and G. Stock, *Phys. Rev. Lett.* **109**, 173201 (2012).
  - [47] J. Eckel, J. H. Reina, and M. Thorwart, *New J. Phys.* **11**, 085001 (2009).
  - [48] The RG flow equations in transformed basis for  $\hat{\Delta}$  with  $\varphi \neq 0$  are identical to that of  $\Delta_0$  with  $\varphi = 0$  [7, 45]:  $\frac{d(\hat{\Delta}/\omega_c)}{d\ell} \approx (1 - \alpha)\hat{\Delta}/\omega_c$  and  $\frac{d\alpha}{d\ell} \approx -\alpha(\hat{\Delta}/\omega_c)^2$ . This ensures that the fixed point ( $\hat{\Delta} \approx 0, \alpha \approx 1$ ) for  $\varphi \neq 0$  and  $\varphi = 0$  remains identical. Consequently, the BKT phase transition for any  $\varphi$  emerges at  $\alpha = \alpha_c = 1 + O(\Delta_0/\omega_c)$ .
  - [49] For ultra-strong coupling ( $\alpha > \alpha_c$ ) and  $\varphi = 0$ , localization implies a degenerate ground state [9, 10]. Specifically, changing the initial condition from  $P_z(t=0) = 1$  to  $P_z(t=0) = -1$ , yields that  $P_z(t \rightarrow \infty) = 1$  changes to  $P_z(t \rightarrow \infty) = -1$ . Such degeneracy is preserved for  $\varphi \neq 0$ : for initial condition from  $P_z(t=0) = \pm 1$ , the system equilibrates to  $P_z(t \rightarrow \infty) = \pm \cos^2 \varphi$ .
  - [50] In molecular systems typical primary mode frequency  $\hat{\Omega} \sim 200 \text{ cm}^{-1}$  [46] and damping coefficient  $\gamma \sim 2500 \text{ cm}^{-1}$  ( $\omega_c = \hat{\Omega}^2/\gamma = 16 \text{ cm}^{-1}$  [47],  $\gamma \gg \hat{\Omega}$  [38]), which gives an oscillations frequency  $\Omega_0 \approx 950 \text{ cm}^{-1}$  (eq. 4) when  $\alpha = 1$  and  $b = 3$ . On the other hand, when  $\alpha = 2.5$  and  $b = 3$ ,  $\Omega_0 \approx 2370 \text{ cm}^{-1}$ .